Published in final edited form as:
J Neurooncol. 2011 August ; 104(1): 55–63. doi:10.1007/s11060-010-0470-8.

Nanoshell-mediated photothermal therapy improves survival in a murine glioma model

Emily S. Day,
Department of Bioengineering, Rice University, 6100 Main Street MS-142, Houston, TX 77005, USA

Patrick A. Thompson,
Texas Children's Cancer Center, Texas Children's Hospital, Baylor College of Medicine, Houston, TX, USA

Linna Zhang,
Texas Children's Cancer Center, Texas Children's Hospital, Baylor College of Medicine, Houston, TX, USA

Nastassja A. Lewinski,
Department of Bioengineering, Rice University, 6100 Main Street MS-142, Houston, TX 77005, USA

Nabil Ahmed,
Texas Children's Cancer Center, Texas Children's Hospital, Baylor College of Medicine, Houston, TX, USA

Rebekah A. Drezek,
Department of Bioengineering, Rice University, 6100 Main Street MS-142, Houston, TX 77005, USA

Susan M. Blaney, and
Texas Children's Cancer Center, Texas Children's Hospital, Baylor College of Medicine, Houston, TX, USA

Jennifer L. West
Department of Bioengineering, Rice University, 6100 Main Street MS-142, Houston, TX 77005, USA

Abstract

We are developing a novel treatment for high-grade gliomas using near infrared-absorbing silica–gold nanoshells that are thermally activated upon exposure to a near infrared laser, thereby irreversibly damaging cancerous cells. The goal of this work was to determine the efficacy of nanoshell-mediated photothermal therapy in vivo in murine xenograft models. Tumors were induced in male Icr-Tac:ICR-Prkdc^{SCID} mice by subcutaneous implantation of Firefly Luciferase-labeled U373 human glioma cells and biodistribution and survival studies were performed. To evaluate nanoparticle biodistribution, nanoshells were delivered intravenously to tumor-bearing mice and after 6, 24, or 48 h the tumor, liver, spleen, brain, muscle, and blood were assessed for gold content by inductively coupled plasma-mass spectrometry (ICP-MS) and histology.

jwest@rice.edu.

Electronic supplementary material The online version of this article (doi:10.1007/s11060-010-0470-8) contains supplementary material, which is available to authorized users.

Nanoshell concentrations in the tumor increased for the first 24 h and stabilized thereafter. Treatment efficacy was evaluated by delivering saline or nanoshells intravenously and externally irradiating tumors with a near infrared laser 24 h post-injection. Success of treatment was assessed by monitoring tumor size, tumor luminescence, and survival time of the mice following laser irradiation. There was a significant improvement in survival for the nanoshell treatment group versus the control ($P < 0.02$) and 57% of the mice in the nanoshell treatment group remained tumor free at the end of the 90-day study period. By comparison, none of the mice in the control group survived beyond 24 days and mean survival was only 13.3 days. The results of these studies suggest that nanoshell-mediated photothermal therapy represents a promising novel treatment strategy for malignant glioma.

Keywords

Glioma; Nanoshells; Thermal therapy; Biodistribution; Survival; In vivo

Introduction

Primary brain tumors represent one of the most challenging forms of neoplasia to treat. High-grade gliomas are the most aggressive type of primary brain tumor and despite medical intervention the median survival is only 12–15 months and 5-year survival is less than 5% [1–4]. Surgery is an acceptable treatment option *if* the tumor location is amenable to removal, but often the infiltrative nature of high-grade gliomas prevents complete resection. Radiation therapy and chemotherapy are also viable treatment options but they are plagued by side effects that range from minor reactions (e.g. nausea, hair loss) to extreme complications such as personality changes, loss of physical ability, or cognitive dysfunction [5, 6]. Therefore, there is a significant need for advances in care not only to improve survival but also to improve quality of life following treatment.

Hyperthermia, the application of heat to destroy solid tumors, has been used as an adjuvant cancer treatment for some time but is not currently utilized as an independent treatment modality. Sources for heat generation, which induces cell death through mechanisms such as protein denaturation and rupture of cellular membranes, include radiofrequency and microwaves, laser light, and ultrasound [7]. Advantages of hyperthermia over conventional treatment include the ease of application, negligible morbidity, and ability to treat deeply embedded tumors where surgery is not feasible. In addition, heat-based mechanisms to induce cell death are less prone to development of cellular resistance. However, widespread use of this technology has been prevented by the inability of simple heating techniques to discern normal from diseased tissue. To overcome this limitation researchers are evaluating strategies that incorporate nanoparticles as exogenous energy absorbers to provide specific delivery of heat selectively to tumors, sparing normal surrounding tissue [8]. Significant success has been achieved in vivo with a variety of nanoparticles, including iron oxide nanoparticles [9–11], gold nanorods [12], carbon nanotubes [13], and silica–gold nanoshells [14, 15].

We have previously demonstrated successful targeted ablation of medulloblastoma and glioma in vitro using antibody-conjugated silica–gold nanoshells [16]. These nanoparticles consist of a spherical silica core of approximately 120 nm diameter surrounded by a thin gold shell (10–20 nm thickness) and they efficiently convert near infrared light energy into heat, enabling their use as photothermal cancer therapeutic agents [17]. The goal of the present study was to expand upon our previous in vitro success by investigating the ability of nanoshell-mediated photothermal therapy to eradicate high-grade glioma in vivo. In an initial biodistribution study, nanoshell accumulation in subcutaneous tumors was monitored

over a 48 h timeframe following intravenous nanoparticle delivery. A subsequent study compared survival of tumor-bearing mice that received nanoshells plus laser irradiation versus control mice that received laser irradiation alone. There was a statistically significant increase in survival for mice in the nanoshell treatment group with more than half of the mice in this group experiencing complete response, suggesting that nanoshell-mediated photothermal therapy may be a viable treatment option for primary brain tumors.

Materials and methods

Synthesis of silica–gold nanoshells

Nanoshells consisting of silica cores and thin gold shells were fabricated following the technique of Oldenburg et al. [18]. Colloidal silica (120 nm diameter, Precision Colloids, Cartersville, GA) functionalized with 3-aminopropyl-triethoxysilane (Gelest, Inc., Morrisville, PA) was decorated with colloidal gold (~3 nm diameter) synthesized according to Duff et al. [19]. The gold shell was completed by reducing additional gold onto these nucleation sites, producing nanoshells with peak absorption at 800 nm and a total diameter of ~150 nm. Nanoshells were visualized with transmission electron microscopy and particle diameter was analyzed using ImageJ software (NIH, Bethesda, MD). To enhance stability, prevent non-specific protein adsorption, and increase circulation time in vivo the nanoshells were coated with poly(ethylene glycol) (PEG) by reacting with mPEG-SH (5000 Da, Nektar, San Carlos, CA) for a minimum of 4 h at 4°C. PEG molecules self-assemble on the nanoshell surface due to dative interactions between sulfur and gold. Nanoshells were centrifuged at 500 g for 5 min to remove unbound PEG molecules and suspended in sterile saline solution (1.7×10^{11} nanoshells/ml) prior to injection in the animals.

Cell preparation

U373 human high-grade glioma cells (ATCC, Manassas, VA) were engineered to constitutively express the firefly luciferase gene to enable imaging of tumor growth in vivo. An MSCV (murine stem cell virus) retroviral vector with a gene encoding the fusion protein eGFP-Firefly Luciferase (eGFP.FFLuc) was used to generate firefly luciferase expressing cells [20]. Cells were seeded at low density in a 6-well plate in a high-titer retroviral supernatant derived from a producer cell line stably transfected to shed these viral particles. Polybrene was used to facilitate viral entry into the U373 cells. This procedure was repeated 2–3 times after which cells were harvested and sorted for eGFP positivity. The intensity of light was tested routinely in a luminometer after 150 mg/kg D-luciferin (Xenogen, Alameda, CA) was added prior to conducting the animal experiments to ensure the uniformity of light emission from the tumor cells.

Murine tumor model

Firefly luciferase expressing U373 cells were maintained in RPMI 1640 medium (Invitrogen Corp., Carlsbad, CA) supplemented with 1% glutamine and 10% fetal bovine serum and cultured at 37°C in a 5% CO_2 environment. Cells were detached from culture flasks with trypsin–EDTA and diluted in culture media for inoculation into mice. All animals were used under an approved protocol of the Institutional Animal Care and Use Committee of Baylor College of Medicine. To induce tumor growth, 10^6 U373 cells were injected subcutaneously in the right hind flank of male IcrTac:ICR-Prkdc^{SCID} mice (Taconic Farms, Hudson, NY). Tumor development was monitored daily by measurement with calipers and with bioluminescent imaging. When tumor diameter reached 3–5 mm the mice received intravenous injections of 100 μl PEG-coated nanoshells (1.7×10^{11} particles/ml) or saline. A total of 9 mice were used in the biodistribution study and 15 mice in the survival experiment.

Bioluminescent imaging

Isoflurane anesthetized animals were imaged using the Xenogen IVIS 100 system (Caliper Life Sciences, Alameda, CA) 10 min after receiving intraperitoneal injections of 150 mg/kg D-luciferin (Xenogen), which emits light when oxidized in the presence of luciferase and ATP. The photons emitted from luciferase-expressing U373 cells within the animal body and transmitted through the tissue were quantified using "Living Image," a software program provided by the same manufacturer. A pseudo-color image representing light intensity (blue least intense and red most intense) was generated and superimposed over the grayscale reference image. Mice were imaged daily following cell implantation to monitor tumor development.

Analysis of nanoshell biodistribution and tumor uptake

A biodistribution study was performed to determine the time of maximum nanoshell accumulation in tumors following intravenous delivery (and thus the optimal time for laser application). Three mice were euthanized at 6, 24, and 48 h post-tail vein injection of nanoshells and the blood, brain, tumor, spleen, liver, and muscle were collected for assessment of gold content. Each tissue specimen (apart from blood) was divided into two pieces—one for qualitative analysis of nanoshell accumulation by histology and one for quantitative analysis with inductively coupled plasma-mass spectrometry (ICP-MS). Blood samples were only tested by ICP-MS.

Preparation of histological specimens—Histological specimens were formalin-fixed, paraffinembedded, cut into 6 μm sections and examined by darkfield microscopy and by hematoxylin and eosin (H&E) staining as well as silver staining. Darkfield imaging was performed on unstained tissue sections using an Axiovert 135 inverted microscope (Carl Zeiss, Thornwood, NJ) coupled to a CytoViva high resolution adaptor (CytoViva, Auburn, AL). With this technique, indirect sample illumination enables image production from light scattered by the samples and nanoshells are easily detected since they have enhanced scattering properties compared to tissue components [21–23]. H&E staining and silver enhancement, which amplifies the size of the nanoshells to allow detection via optical microscopy by utilizing the nanoparticles as nucleation sites for the deposition of silver, was also employed to confirm nanoshell presence. Samples were deparaffinized, stained with a Silver Enhancer Kit (KPL, Gaithersburg, MD), rinsed, and counterstained with hematoxylin and eosin Y to show cell nuclei and cytoplasm. For H&E staining, samples were exposed to hematoxylin, washed with water and ethanol, stained with eosin Y, rinsed with ethanol and xylene and mounted for microscopy.

Preparation of samples for inductively coupled plasma-mass spectrometry—Samples for ICP-MS were lyophilized, weighed, and digested with 0.5 ml aqua regia under mild heating conditions (~60°C). Trace grade nitric acid and hydrochloric acid were purchased from Sigma-Aldrich (St. Louis, MO) and VWR (West Chester, PA), respectively. Digested samples were diluted with 1% aqua regia to 10 ml and filtered through a 0.45 μm filter. Standard solutions of known gold concentrations were prepared in 1% aqua regia using certified reference material Gold Standard for ICP (Sigma-Aldrich). The standards and samples were analyzed for ^{197}Au with germanium as an internal standard using the ELAN 9000 ICP-MS from Perkin-Elmer (Waltham, MA).

In vivo photothermal therapy

After the biodistribution study confirmed that nanoshells delivered via the tail vein accumulated in subcutaneous U373 tumors, a survival study was carried out to evaluate the effectiveness of nanoshell-mediated photothermal therapy in vivo. Tumor-bearing mice

received intravenous injections of 100 μl PEG-coated nanoshells (1.7×10^{11} particles/ml, $n = 7$ mice) or saline ($n = 8$ mice) when tumor diameter reached 3–5 mm. Following a 24 h circulation period mice were anesthetized with sodium pentobarbital (50 mg/kg, intraperitoneal injections) and tumors were swabbed with glycerol as an index matching agent prior to transdermal irradiation for 3 min with an 800 nm diode laser (Coherent, Inc., Santa Clara, CA) set to an intensity of 4 W/cm^2 (spot diameter = 9 mm). Tumor length and width were measured with digital calipers daily following treatment to track growth or regression. Tumor development was also monitored with bioluminescent imaging as described above. Since photon flux from the tumor is proportional to the number of light emitting cells, the signal intensity is indicative of response to treatment. Mice were monitored for 90 days or until tumors reached 10 mm in largest diameter, at which point they were euthanized by carbon dioxide asphyxiation.

Statistical analysis

Survival results were expressed as a Kaplan–Meier curve and survival between treatment and control groups was compared using a logrank test with calculations performed in MedCalc Software (Mariakerke, Belgium). Differences in survival were considered significant for $P < 0.05$.

Results

Nanoshell synthesis

Silica–gold nanoshells fabricated as described above had a peak plasmon resonance at 800 nm. Figure 1 displays the extinction spectrum of the nanoshells with a transmission electron micrograph shown in the inset. Using TEM images, particle diameter was measured with ImageJ software (NIH, Bethesda, MD) and analysis of 50 nanoshells indicated the average particle diameter was 152.0 ± 8.8 nm.

Biodistribution of nanoshells in tumor-bearing mice

No adverse effects of nanoshell injections were observed at the delivery site or systemically in these experiments. Uptake of nanoshells by tumor and other organs was assessed through both quantitative and qualitative techniques and the results were in good agreement.

ICP-MS analysis of gold content demonstrated nanoshell accumulation in tumors—Inductively coupled plasma-mass spectrometry (ICP-MS) has been demonstrated as an effective method for determining gold content in tissue specimens [24–26]. In our study we calculated the mean and standard deviation of gold content in each organ from samples of three mice at 6, 24, and 48 h post-intravenous delivery of nanoshells (Fig. 2, Supplemental Table 1). Measurement of gold content by ICP-MS indicated that the intratumoral nanoshell concentration increased for the first 24 h following tail vein delivery and stabilized at ~50 ppm (μg gold/g dry tissue) thereafter (Table 1). The amount of gold in the tumor 24 h post-injection was 35 times higher than the concentration in muscle adjacent to the tumor, so collateral damage to normal tissue regions surrounding the tumor was anticipated to be minimal during photothermal therapy. Nanoshell clearance from the blood followed an exponential decay with a calculated circulation half-life of 4.8 h, comparable to the 4.1 h half-life of nanoshells determined by Xie et al. [27]. We observed a pronounced level of gold in the liver and spleen, two organs associated with the reticuloendothelial system. In general, the gold content we determined to be present in each organ by ICP-MS followed the trends observed by James et al., who used neutron activation analysis to assess biodistribution of 130 nm diameter nanoshells in healthy and tumor-bearing mice [28].

Darkfield microscopy and histology corroborated ICP-MS results—Darkfield imaging of unstained tissue sections provided a visual confirmation of the ICP-MS findings. Nanoshells appeared red against the blue-gray tissue background due to their enhanced ability to scatter light, and were present at high levels in the spleen, liver, and tumor (Fig. 3). Nanoshells were not readily observed in the brain and muscle by darkfield microscopy which was expected given that ICP-MS indicated gold content in these tissues was less than 5 ppm (μg gold/g dry tissue) at all timepoints. Additional tissue sections were stained with hematoxylin and eosin and silver enhancement solution to show tissue structure and confirm nanoshell presence and the results further corroborated the ICP-MS data. Nanoshells appear brown-to-black against the tissue background and qualitative analysis did not reveal any adverse reactions of organs to nanoshell presence (Fig. 4).

Animal survival following photothermal therapy

Based on the conclusions of the biodistribution study, laser exposure was performed 24 h post-tail vein delivery of nanoshells to give the nanoparticles sufficient time to accumulate in subcutaneous U373 tumors. Following laser irradiation mice were monitored daily to track tumor growth and regression using bioluminescent imaging and caliper measurements to indicate cellular development and changes in size. When the tumor reached 10 mm in largest diameter the mice were euthanized. Nanoshell-mediated photothermal therapy induced tumor regression and led to improved survival versus control animals.

Bioluminescent imaging indicated nanoshell-mediated photothermal therapy induced tumor regression—Bioluminescent imaging of tumors following laser irradiation helped distinguish each animal's response to therapy, with some mice experiencing complete response to treatment while others exhibited partial or non-response (Fig. 5). The mouse shown in the first row of Fig. 5 received nanoshell-assisted laser therapy and displayed complete tumor regression without signs of re-growth for the entire period of study. This mouse had a visible scab and loss of luminescence in the location of the tumor within just 3 days of treatment. The presence of a scab is indicative of the intense local heat generated by nanoshells within the tumor during laser irradiation; similar blemishes were not seen on mice that received laser irradiation only. The mouse in the second row also received nanoshell-mediated photothermal therapy and is an example of a partial responder, evidenced by initial loss in signal intensity during the first week following laser irradiation and subsequent reappearance of tumor cell luminescence by day 20 post-irradiation. The third row shows a mouse from the control group in which signal intensity and tumor burden increased continually following laser irradiation. This response pattern was typical for all mice in the control group.

Nanoshell-mediated photothermal therapy improved survival—Survival probability was another metric used to evaluate the effectiveness of therapy. Figure 6 is a Kaplan–Meier diagram showing the percentage of mice still alive versus time following laser irradiation for both the nanoshell treatment and laser only control groups. Analysis with a logrank test revealed that the two survival curves differed significantly ($P = 0.0155$) and it can be concluded that nanoshell-mediated photothermal therapy has a significant influence on survival time. Tumors progressed rapidly in the control group and none of the eight mice survived beyond 24 days (mean survival = 13.3 days); by comparison, four of seven mice in the nanoshell therapy group survived for the entire 90 day period of study (overall survival = 57%) and each of these mice were completely tumor free without sign of recurrence at that time.

Discussion

The prognosis for patients with high-grade glioma remains dismal with conventional multi-modality treatment techniques indicating an urgent need for novel therapeutic advances [29]. Hyperthermia is an attractive therapeutic approach; however, currently available simple heating techniques cannot distinguish normal from diseased tissue. To circumvent this problem, exogenous tumor-targeted heating agents (such as silica–gold nanoshells, nanorods, magnetic nanoparticles, and carbon nanotubes) have been employed to provide specific heating of diseased regions while minimizing thermal insult to normal tissue. Nanoshell-assisted photothermal therapy has demonstrated effectiveness against a variety of tumors in preclinical studies, with 80–100% survival in murine models of colon carcinoma [14, 15] and in vitro successes against breast [30], prostate [23], and brain [16] tumor cell lines. The ability to heat nanoshell-laden tumors but not white matter in a canine brain metastasis model has also been reported [31]. Our aim in this work was to expand upon previous research by testing nanoshell-mediated photothermal therapy as a tool for management of glioma, a highly infiltrative primary brain tumor. The ideal treatment strategy for malignant gliomas is one that produces minimal collateral damage to the surrounding central nervous system structures.

Our results suggest that nanoshell-mediated photothermal therapy is a safe and effective method for destruction of glioma in vivo. Nanoshell-mediated photothermal therapy resulted in a statistically significant increase in survival, an exciting result given the exceedingly invasive nature of this type of tumor. In addition, it is highly encouraging that more than half of the mice in the nanoshell treatment group displayed complete tumor regression following only one laser treatment, and it is possible that multiple exposures could further increase the therapeutic benefit. The only reaction to laser ablation of the tumor observed was presence of a scab that healed naturally over time, which indicated the extreme heat-producing capability of nanoshells. Appearance of similar skin changes have been reported during thermal therapy with carbon nanotubes [13], but this is a relatively minor side effect compared to those from conventional therapy, which can range from chemotherapy-induced nausea to extreme changes in personality or cognitive capacity induced by surgery or radionecrosis. Nevertheless, in the clinical setting it will be necessary to monitor temperature changes during the course of nanoshell-mediated photothermal therapy in order to prevent unwanted damage to normal brain tissue. This can be accomplished using magnetic resonance thermal imaging, as previously described by Schwartz et al. [31]. With temperature carefully monitored, magnetic fluid hyperthermia was well-tolerated in a feasibility study reported by Maier-Hauff et al. with only minor side effects observed [9], so it is expected that thermal therapy mediated by nanoshells would elicit similar responses with minimal side effects.

One advantage of nanoparticles activated by a magnetic field is the ability to treat deeply embedded tumors without the need for invasive procedures, as the strength of the applied magnetic field is not attenuated by passage through the body. By comparison, light cannot penetrate the human skull so treatment of human brain tumors with nanoshell-mediated photothermal therapy will likely require use of fiber optic laser probes to deliver the light energy. Very large tumors might require multiple procedures or application of the laser from several directions to ensure damage throughout the tumor volume. While this will increase the invasiveness of the procedure, it does offer the benefit that laser irradiation (and thus thermal therapy) can be delivered to very specific locations, thereby minimizing offtarget effects. Schwartz et al. have previously demonstrated the feasibility of using fiber optic probes for nanoshell-mediated thermal therapy of a canine brain tumor model [31]. Based on this research, we believe the use of fiber optic probes could be translated to treatment of glioma. Interstitial light delivery is currently being investigated in an ongoing Phase I

clinical trial for treatment of head and neck cancer, and this study will help determine the applicability of this approach [32]. It should be noted that the combined use of directed laser energy and accurate temperature monitoring (such as with magnetic resonance thermal imaging) would help circumvent one of the limitations of hyperthermia, which is lack of control over the vascular environment of the tumor. For example, although increased vessel density would provide enhanced nanoshell deposition it may also induce more rapid cooling due to blood flow; since effective therapy requires a precise balance of nanoshell dosage and applied laser energy, temperature monitoring during therapy could help guide decisions regarding these parameters to ensure even heat distribution throughout the tumor.

Histology and ICP-MS revealed that nanoshells delivered intravenously were selectively located in tumors and not adjacent muscle, which is highly desirable for the minimization of thermal damage to adjacent healthy tissue. Low nanoshell concentrations were also found in normal brain, which is advantageous since heating of vital areas in this organ should be avoided. Since most highly malignant central nervous system (CNS) tumors have disrupted blood–brain barriers (BBBs) at presentation, nanoshell penetration into the tumor should be adequate as previously demonstrated by successful intravenous delivery of PEG-coated nanoshells to intracranial tumors in a canine model [31]. In cases where PEG-coated nanoshells do not extravasate across the BBB at levels sufficient for effective heating, tumor accumulation may be enhanced by targeting tumor antigens or tumor vasculature with antibody-coated nanoshells. The ability to target medulloblastoma and glioma cells with antibody-coated nanoshells has previously been demonstrated in vitro [16], and we are currently assessing this technique in vivo in orthotopic xenografts. Alternatively, nanoshells could be injected directly into tumors but this would increase the invasiveness of the therapeutic approach, which is generally undesirable.

No adverse response to nanoshell presence in the body was observed in the timeframe examined, though the effects of prolonged or repeated exposure remain to be investigated. A few studies have briefly examined safety but the timeframe remains on the order of months. For example, James et al. found that nanoshells persist in the body up to 28 days post injection without toxicity [28], and O'neal et al. reported that mice remain healthy greater than 90 days post therapy [14], consistent with our findings. There is currently no evidence that nanoshells are degraded by the body and the laser energies used in treatment are much lower than the energy required to break the particles down to their component parts, so it is anticipated that nanoshells' long-term compatibility will be largely determined by the surface characteristics and gold has been used clinically for many decades. An initial assessment of nanoshell safety in humans will be gained from the ongoing Phase I clinical trial of nanoshell-mediated photothermal therapy for treatment of head and neck cancer [32]. Given the dismal prognosis and life expectancy for children and adults with high-grade glioma, innovative treatment approaches must be explored and the risk/benefit ratio carefully assessed.

In summary, we have demonstrated the effectiveness of nanoshell-mediated photothermal therapy against glioblastoma in vivo using a subcutaneous murine tumor model. Nanoshells delivered intravenously accumulated in subcutaneous tumors at levels sufficient to induce destructive heating of cancerous cells upon transdermal irradiation with a near infrared laser. Treatment led to subsequent tumor regression and improved overall survival versus control mice that received laser irradiation alone. These results warrant further investigation of nanoshell-mediated photothermal therapy for treatment of primary brain tumors and studies using orthotopic tumor models are currently ongoing. These orthotopic models will be important for validation of the technique not only because of need to verify nanoshell passage through the blood–brain barrier and accumulation in tumors, but also because microenvironment plays a critical role in tumor cell behavior and may influence response to

treatment. In addition, these studies will elucidate whether adjustments need to be made to particle concentration or laser parameters to accommodate for attenuation of light as it passes through the skull. In the future, this novel approach to cancer therapy could yield a promising alternative to conventional treatment modalities.

Supplementary Material

Refer to Web version on PubMed Central for supplementary material.

Acknowledgments

The authors would like to thank Ying Hu of Rice University for assistance with transmission electron microscopy.

Funding Funding was provided by a grant from Hope Street Kids to P.A.T; National Science Foundation (EEC-0647452 to J.L.W., Graduate Research Fellowship to E.S.D); National Institutes of Health (R21 CA118788 to J.L.W, MSCIDA 3 U10 HD037242-08S1 to P.A.T.).

References

1. Gladson CL, Prayson RA, Liu WM. The pathobiology of glioma tumors. Annu Rev Pathol. 2010; 5:33–50. [PubMed: 19737106]
2. Stupp R, Mason WP, van den Bent MJ, et al. Radiotherapy plus concomitant and adjuvant temozolomide for glioblastoma. N Engl J Med. 2005; 352(10):987–996. [PubMed: 15758009]
3. Wen PY, Kesari S. Malignant gliomas in adults. N Engl J Med. 2008; 359(5):492–507. [PubMed: 18669428]
4. Daumas-Duport C, Scheithauer B, Ofallon J, Kelly P. Grading of astrocytomas-a simple and reproducible method. Cancer. 1988; 62(10):2152–2165. [PubMed: 3179928]
5. Butler JM, Rapp SR, Shaw EG. Managing the cognitive effects of brain tumor radiation therapy. Curr Treat Options Oncol. 2006; 7(6):517–523. [PubMed: 17032563]
6. Ricard D, Taillia H, Renard JL. Brain damage from anti-cancer treatments in adults. Curr Opin Oncol. 2009; 21(6):559–565. [PubMed: 19667984]
7. Wust P, Hildebrandt B, Sreenivasa G, Rau B, Gellermann J, Riess H, Felix R, Schlag PM. Hyperthermia in combined treatment of cancer. Lancet Oncol. 2002; 3(8):487–497. [PubMed: 12147435]
8. Day ES, Morton JG, West JL. Nanoparticles for thermal cancer therapy. J Biomech Eng-Trans ASME. 2009; 131(7):5. 074001.
9. Maier-Hauff K, Rothe R, Scholz R, Gneveckow U, Wust P, Thiesen B, Feussner A, von Deimling A, Waldoefner N, Felix R, Jordan A. Intracranial thermotherapy using magnetic nanoparticles combined with external beam radiotherapy: results of a feasibility study on patients with glioblastoma multiforme. J Neurooncol. 2007; 81(1):53–60. [PubMed: 16773216]
10. Wust P, Gneveckow U, Johannsen M, Bohmer D, Henkel T, Kahmann F, Sehouli J, Felix R, Ricke J, Jordan A. Magnetic nanoparticles for interstitial thermotherapy—feasibility, tolerance and achieved temperatures. Int J Hyperth. 2006; 22(8):673–685.
11. Jordan A, Scholz R, Maier-Hauff K, van Landeghem FKH, Waldoefner N, Teichgraeber U, Pinkernelle J, Bruhn H, Neumann F, Thiesen B, von Deimling A, Felix R. The effect of thermotherapy using magnetic nanoparticles on rat malignant glioma. J Neurooncol. 2006; 78(1): 7–14. [PubMed: 16314937]
12. Dickerson EB, Dreaden EC, Huang XH, El-Sayed IH, Chu HH, Pushpanketh S, McDonald JF, El-Sayed MA. Gold nanorod assisted near-infrared plasmonic photothermal therapy (PPTT) of squamous cell carcinoma in mice. Cancer Lett. 2008; 269(1):57–66. [PubMed: 18541363]
13. Moon HK, Lee SH, Choi HC. In vivo near-infrared mediated tumor destruction by photothermal effect of carbon nanotubes. ACS Nano. 2009; 3(11):3707–3713. [PubMed: 19877694]
14. O'Neal DP, Hirsch LR, Halas NJ, Payne JD, West JL. Photo-thermal tumor ablation in mice using near infrared-absorbing nanoparticles. Cancer Lett. 2004; 209(2):171–176. [PubMed: 15159019]

15. Gobin AM, Lee MH, Halas NJ, James WD, Drezek RA, West JL. Near-infrared resonant nanoshells for combined optical imaging and photothermal cancer therapy. Nano Lett. 2007; 7(7): 1929–1934. [PubMed: 17550297]

16. Bernardi RJ, Lowery AR, Thompson PA, Blaney SM, West JL. Immunonanoshells for targeted photothermal ablation in medulloblastoma and glioma: an in vitro evaluation using human cell lines. J Neurooncol. 2008; 86(2):165–172. [PubMed: 17805488]

17. Hirsch LR, Stafford RJ, Bankson JA, Sershen SR, Rivera B, Price RE, Hazle JD, Halas NJ, West JL. Nanoshell-mediated near-infrared thermal therapy of tumors under magnetic resonance guidance. Proc Natl Acad Sci USA. 2003; 100(23):13549–13554. [PubMed: 14597719]

18. Oldenburg SJ, Averitt RD, Westcott SL, Halas NJ. Nano-engineering of optical resonances. Chem Phys Lett. 1998; 288(2–4):243–247.

19. Duff DG, Baiker A, Edwards PP. A new hydrosol of gold clusters. 1. Formation and particle-size variation. Langmuir. 1993; 9(9):2301–2309.

20. Ahmed N, Ratnayake M, Savoldo B, Perlaky L, Dotti G, Wels WS, Bhattacharjee MB, Gilbertson RJ, Shine HD, Weiss HL, Rooney CM, Heslop HE, Gottschalk S. Regression of experimental medulloblastoma following transfer of her2-specific t cells. Cancer Res. 2007; 67(12):5957–5964. [PubMed: 17575166]

21. Loo C, Hirsch L, Lee MH, Chang E, West J, Halas N, Drezek R. Gold nanoshell bioconjugates for molecular imaging in living cells. Opt Lett. 2005; 30(9):1012–1014. [PubMed: 15906987]

22. Loo C, Lowery A, Halas N, West J, Drezek R. Immunotargeted nanoshells for integrated cancer imaging and therapy. Nano Lett. 2005; 5(4):709–711. [PubMed: 15826113]

23. Gobin AM, Moon JJ, West JL. Ephrin AI-targeted nanoshells for photothermal ablation of prostate cancer cells. Int J Nanomed. 2008; 3(3):351–358.

24. De Jong WH, Hagens WI, Krystek P, Burger MC, Sips A, Geertsma RE. Particle size-dependent organ distribution of gold nanoparticles after intravenous administration. Biomaterials. 2008; 29(12):1912–1919. [PubMed: 18242692]

25. Sonavane G, Tomoda K, Makino K. Biodistribution of colloidal gold nanoparticles after intravenous administration: effect of particle size. Colloids Surf B Biointerfaces. 2008; 66(2):274–280. [PubMed: 18722754]

26. Niidome T, Yamagata M, Okamoto Y, Akiyama Y, Takahashi H, Kawano T, Katayama Y, Niidome Y. Peg-modified gold nanorods with a stealth character for in vivo applications. J Control Release. 2006; 114(3):343–347. [PubMed: 16876898]

27. Xie H, Gill-Sharp KL, O'Neal DP. Quantitative estimation of gold nanoshell concentrations in whole blood using dynamic light scattering. Nanomedicine. 2007; 3(1):89–94. [PubMed: 17379173]

28. James WD, Hirsch LR, West JL, O'Neal PD, Payne JD. Application of INAA to the build-up and clearance of gold nanoshells in clinical studies in mice. J Radioanal Nucl Chem. 2007; 271(2): 455–459.

29. DeAngelis LM. Brain tumors. N Engl J Med. 2001; 344(2):114–123. [PubMed: 11150363]

30. Lowery AR, Gobin AM, Day ES, Halas NJ, West JL. Immunonanoshells for targeted photothermal ablation of tumor cells. Int J Nanomed. 2006; 1(2):149–154.

31. Schwartz JA, Shetty AM, Price RE, Stafford RJ, Wang JC, Uthamanthil RK, Pham K, McNichols RJ, Coleman CL, Payne JD. Feasibility study of particle-assisted laser ablation of brain tumors in orthotopic canine model. Cancer Res. 2009; 69(4):1659–1667. [PubMed: 19208847]

32. ClinicalTrials.gov [Internet]. National Library of Medicine (US); Bethesda (MD): Feb 29. 2000 p. 4Identifier NCT00848042, pilot study of AuroLase™ therapy in refractory and/or recurrent tumors of the head and neckhttp://clinicaltrials.gov/ct2/show/NCT00848042 [updated 2010 Feb 2cited 2010 Sept 9]

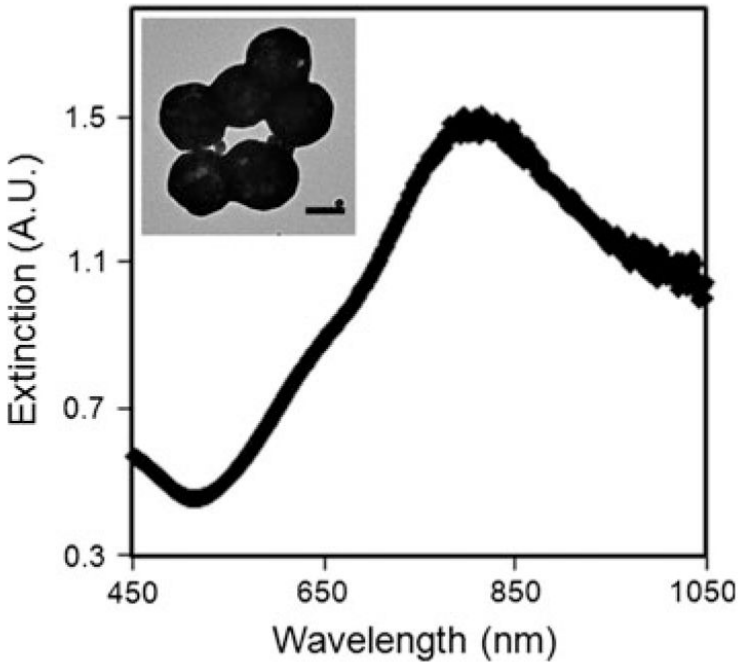

Fig. 1.
Extinction profile of silica–gold nanoshells with peak absorbance at 800 nm. Inset displays a transmission electron micrograph of the nanoparticles. *Scale bar* = 100 nm

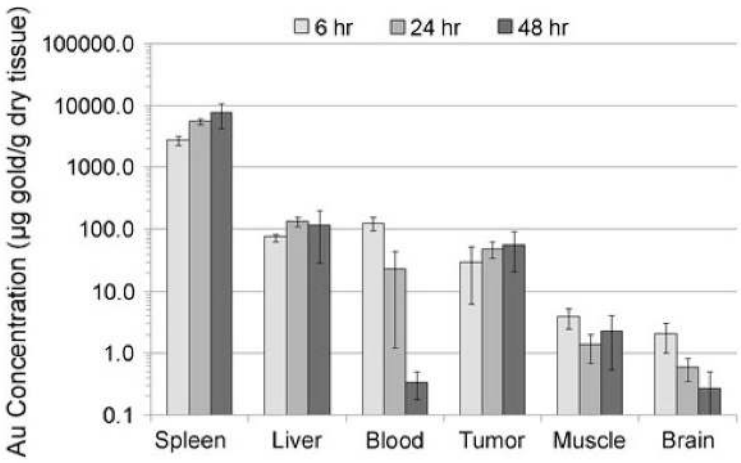

Fig. 2.

Gold distribution to six different organs at 6, 24, and 48 h post-nanoshell delivery via the tail vein determined by ICP-MS. Data depicts mean ± standard deviation for $n = 3$ samples

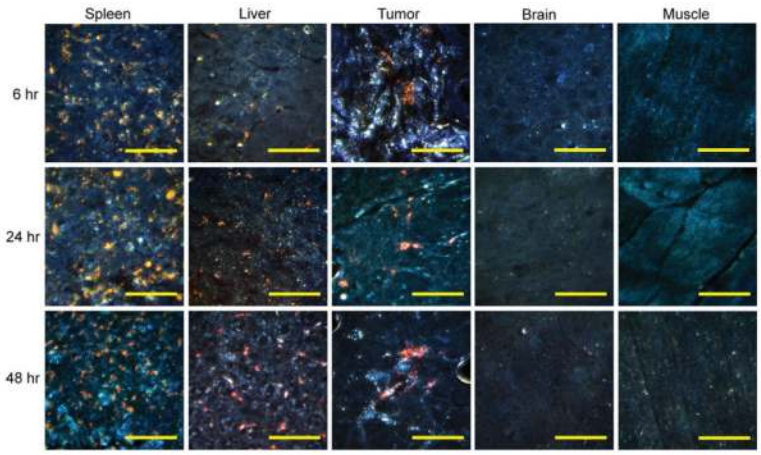

Fig. 3.

Darkfield imaging of tissue sections enabled visualization of nanoshells which appear red due to enhanced light scattering against the blue-gray tissue background. Nanoshells are visible in the spleen, liver, and tumor, but not in the brain and muscle. *Scale bar* = 50 μm

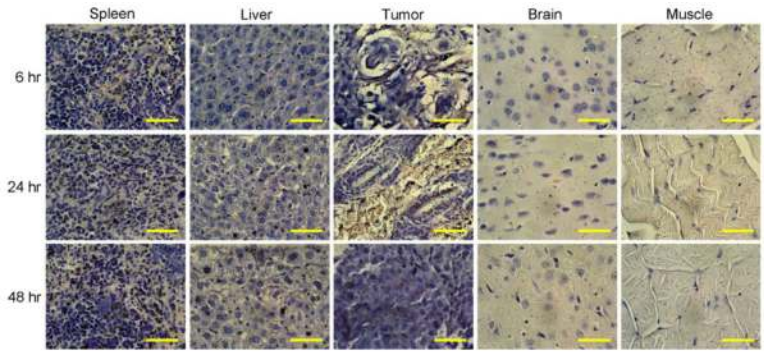

Fig. 4.

Tissue excised 6, 24, and 48 h post-nanoshell delivery was stained with hematoxylin and eosin and silver enhancer to show structure and nanoshells, respectively. Nanoshells appear dark brown or black and are present most abundantly in the spleen, liver, and tumor. *Scale bar* = 50 μm

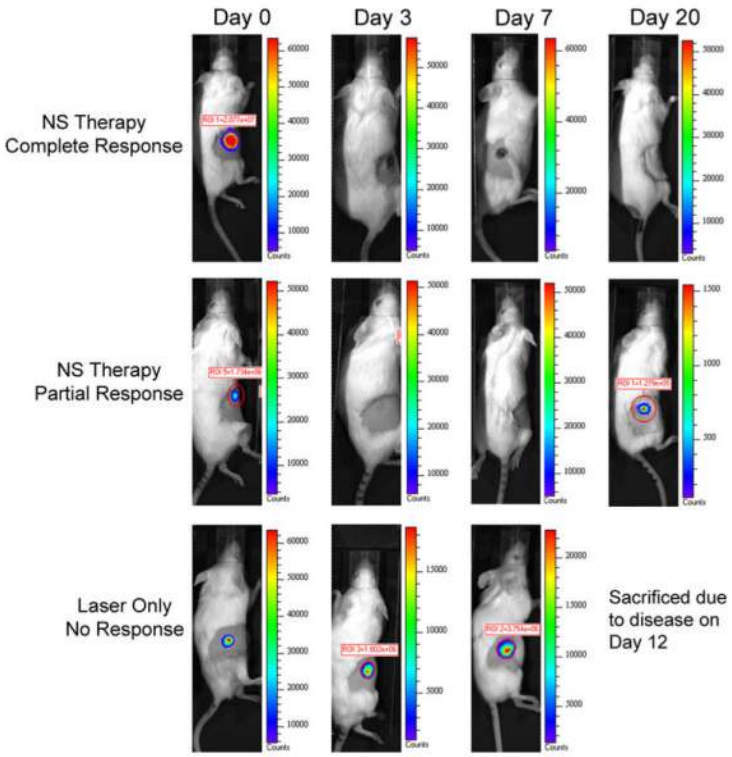

Fig. 5.

Bioluminescent imaging of tumors following laser irradiation. The mouse in the first row displayed loss of luminescence within 3 days of nanoshell therapy and remained tumor-free for the remainder of the study. The mouse in the second row experienced partial response to nanoshell therapy evidenced by initial loss in signal intensity but the tumor later recurred. The third row shows a mouse from the control group in which signal intensity and tumor burden increased following laser irradiation

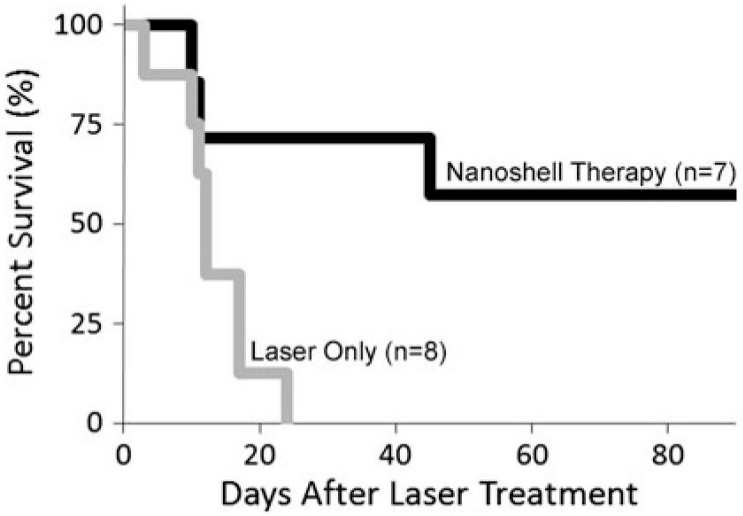

Fig. 6.

Survival versus time for the nanoshell therapy group (*black line*) and the laser control group (*gray line*) for the 90 day period of study. The mean survival time for the control group was 13 days and none of the eight mice survived beyond 24 days. By comparison, four of seven mice (57%) in the treatment group were still alive and tumor-free at day 90 post-irradiation. Analysis with a logrank test revealed a significant improvement in survival with nanoshell-mediated photo-thermal therapy ($P = 0.0155$)

Table 1

Gold concentration in tumor versus time determined by ICP-MS

Time (h)	Mean ± standard deviation (μg gold/g dry tissue)
6	29.5 ± 23.2
24	49.3 ± 13.8
48	56.6 ± 35.4

Intratumoral nanoshell concentrations increased for the first 24 h following tail vein injection of the nanoparticles and stabilized at ~50 ppm (μg gold per g dry tissue) thereafter. Data shows mean and standard deviation of $n = 3$ samples at each timepoint